⌘ *Author's Choice*

THE JOURNAL OF BIOLOGICAL CHEMISTRY VOL. 284, NO. 10, pp. 6260–6269, March 6, 2009

Erythrocytic Casein Kinase II Regulates Cytoadherence of *Plasmodium falciparum*-infected Red Blood Cells*

Received for publication, December 29, 2008 Published, JBC Papers in Press, January 8, 2009, DOI 10.1074/jbc.M809756200

Rachna Hora[‡], Daniel J. Bridges[§], Alister Craig[§], and Amit Sharma[‡1]

From the [‡]Structural and Computational Biology Group, International Centre for Genetic Engineering and Biotechnology, Aruna Asaf Ali Road, New Delhi 110067, India and the [§]Liverpool School of Tropical Medicine, Pembroke Place, Liverpool L3 5QA, United Kingdom

Plasmodium falciparum **malaria is a major human health scourge and a key cause of mortality. Its pathogenicity partly results from the phenomenon of "cytoadherence" mediated by the PfEMP1 (*Plasmodium falciparum* erythrocyte membrane protein 1) family. Extracellular domains of PfEMP1s are variable and bind various host endothelial receptors, whereas their cytoplasmic domains (VARCs) are relatively conserved. VARCs affix PfEMP1s in the human erythrocyte membrane by interacting with host cytoskeleton proteins and exported parasite proteins. Here, we provide *in vitro* and *in vivo* evidence for PfEMP1 phosphorylation (on VARC) and propose an important function for this modification. Specific inhibitors and enhancers have been used to identify erythrocytic casein kinase II (CKII) as the enzyme responsible for VARC modification activity. We have also delineated probable CKII target residues on VARC, which mainly reside in an N-terminal acidic cluster. Our data show that VARC phosphorylation alters its binding to parasite encoded knob-associated histidine-rich protein (KAHRP). Finally, we demonstrate reduced cytoadherence of infected RBCs to endothelial receptors like ICAM-1 and CSA (these contribute to cerebral and placental malaria, respectively) in response to their CKII inhibition. Collectively, this study furthers our understanding of VARC function, underscores the importance of erythrocytic CKII in cytoadherence, and suggests a possible new target for anti-cytoadherence molecules.**

Malaria is a global health problem responsible for ~1 million deaths annually (1). *Plasmodium falciparum* manifests some of its pathogenicity by the phenomenon of cytoadherence, the binding of infected RBCs[2] (iRBCs) to vascular endothelium and their sequestration in the microvasculature of various organs to avoid splenic clearance. Cytoadherence is mediated by the antigenically diverse PfEMP1 family of membrane proteins (encoded by *var* genes), which are ~200–350 kDa in size (2, 3).

Each parasite expresses only one of the ~60 copies of its *var* genes and exports it for insertion into the erythrocyte membrane (2, 3), where it clusters over knobs (4). The extracellular domains of PfEMP1 are variable and interact with a plethora of receptors (CD36, ICAM-I, CSA, etc.) on host cells (5–7). However, their C-terminal cytoplasmic domains (VARCs) of 390–500 amino acids are well conserved and highly acidic (3). VARCs are known to interact with host cytoskeletal proteins actin, spectrin, and actin-spectrin junctions (8). Also, these bind to parasite-encoded KAHRP (8), which forms an essential and major component of the knob structure (9–11). VARC is thus believed to anchor PfEMP1 at the membrane of iRBCs by forming a meshwork of host and parasite proteins that would aid to strengthen and stabilize the roots of PfEMP1-endothelial receptor interaction. Waller *et al.* (12, 13) have mapped the subdomains of PfEMP1 that interact with KAHRP and *vice versa*. Briefly, the histidine-rich subdomain K1A (of KAHRP) strongly interacts with the C-terminal end of VARC, and the highly basic subdomain K2A (of KAHRP; pI = 10.8) has strong affinity for the N-terminal end of VARC. Another report had suggested that the binding between VARC and KAHRP is likely to be driven by electrostatic interactions (14).

Ultrastructural studies have revealed that knobs are electron-dense protrusions on the surface of parasitized erythrocytes that act as focal points of attachment between sequestered iRBCs and host endothelia (15). Knobless parasites generated by disruption of the KAHRP gene (K−) are defective in their ability to cytoadhere under flow conditions, although they are capable of adhering at normal levels when tested in static assays (9). Binding competition experiments between knobby (K+) and K− infected erythrocytes suggested that K+ cytoadherence is of higher affinity than that of K− parasites (16). This reduced adhesiveness of knobless parasites can probably be interpreted as a result of poor anchoring of PfEMP1 to the host membrane by VARC in the absence of KAHRP. However, another report attributes these effects to reduced presentation of PfEMP1 on the surface of knobless iRBCs (17).

Our current studies indicate that PfEMP1 is phosphorylated on its cytoplasmic tail by erythrocytic CKII. This post-translational modification activity is reduced by specific CKII inhibitors and increased by polyamines, which act as specific CKII enhancers. Our biochemical and biophysical data suggest that phosphorylation may induce small and subtle structural changes in VARC. We show that the binding of VARC to KAHRP domains is enhanced significantly upon phosphorylation. Finally, we provide data to show that cell-permeable CKII

* The costs of publication of this article were defrayed in part by the payment of page charges. This article must therefore be hereby marked "*advertisement*" in accordance with 18 U.S.C. Section 1734 solely to indicate this fact.

⌘ *Author's Choice*—Final version full access.

[1] To whom correspondence should be addressed. Tel./Fax: 91-11-26741731; E-mail: amit.icgeb@gmail.com.

[2] The abbreviations used are: RBC, red blood cell; iRBC, infected RBC; KAHRP, knob-associated histidine-rich protein; BSA, bovine serum albumin; DAPI, 4′,6-diamidino-2-phenylindole; ICAM, intercellular adhesion molecule; PBS, phosphate-buffered saline; FL, full-length; CSA, chondroitin sulfate A; TBB, 4,5,6,7-tetrabromotriazole; DMAT, 2-dimethylamino-4,5,6,7-tetrabromo-1*H*-benzimidazole; TBCA, tetrabromocinnamic acid.

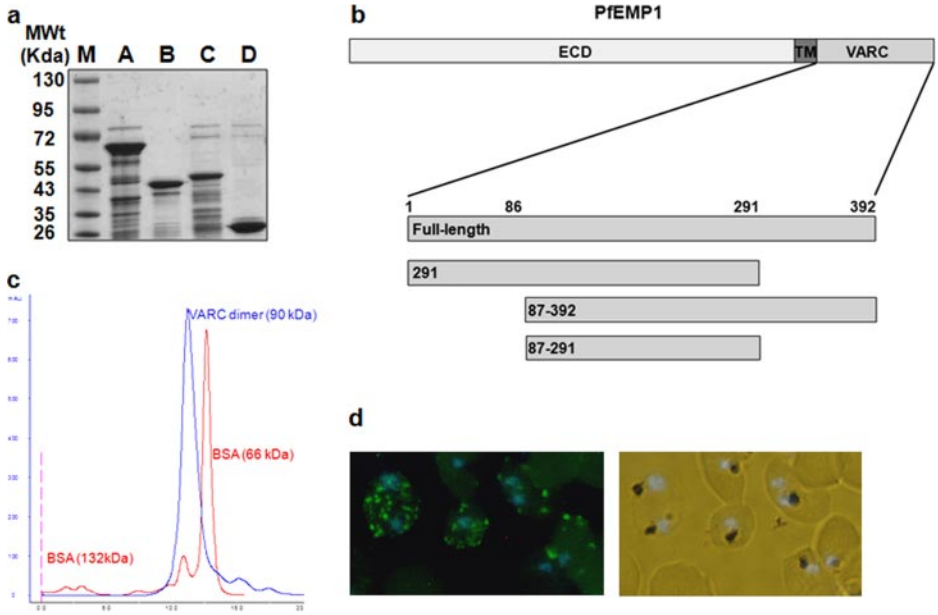

FIGURE 1. **Expression and characterization of PF08_0141 VARC constructs.** *a*, purified VARC and its deletion constructs (5 μg each) loaded on 12% SDS-PAGE. *M*, protein molecular weight marker; *A*, VARC full-length; *B*, VARC 1–291; *C*, VARC 87–392; *D*, VARC 87–291. All constructs were affinity-purified using Ni^{2+}-nitrilotriacetic acid column chromatography, anion-exchanged on Q-Sepharose, and sized by gel exclusion chromatography. *b*, a schematic representation of PfEMP1 organization. The protein comprises an extracellular domain (*ECD*), a transmembrane region (*TM*), and VARC (with its deletion constructs drawn to scale). *c*, determination of oligomeric state of VARC full-length using gel permeation chromatography. VARC full-length and BSA profiles on an S200 Superdex column (GE healthcare) are overlapped to show the dimeric nature of VARC. Peaks corresponding to VARC and BSA (dimer and monomer) are labeled. *d*, immunofluorescence analysis of VARC in mature trophozoites. Methanol-fixed parasitized erythrocytes reacted with mouse anti-VARC antibody (1:1000), fluorescein isothiocyanate-conjugated anti-mouse antibodies (1:2000), and DAPI (0.1 μM). The labeled parasites were photographed using a fluorescence microscope (Nikon) at $\times$40 magnification. The *left panel* shows fluorescence for VARC (*green*), counterstained for nuclei with DAPI (*blue*); the *right panel* shows the corresponding bright field + DAPI.

inhibitors have an impact on cytoadherence of cultured parasitized erythrocytes to host receptors. Together, these observations lead us to hypothesize a model for possible intracellular events in iRBCs at the time of cytoadhesion and propose a likely target for anti-cytoadhesion molecules useful in severe malaria.

EXPERIMENTAL PROCEDURES

Cloning, Expression, and Purification of Recombinant Proteins—Full-length VARC (PF08_0141) was PCR-amplified from 3D7 *P. falciparum* cDNA using *Pfu* polymerase and cloned into pET28a vector. Deletion constructs for VARC (VARC 1–291, 87–392, and 87–291) were PCR-amplified using full-length VARC as a template and cloned into pET28a vector. Residues Thr^{61}, Thr^{64}, Ser^{65}, Ser^{66}, and Ser^{68} in the VARC 1–291 construct were mutated to alanine by site-directed mutagenesis using the QuikChange II kit from Stratagene to generate an N-terminal acidic cluster mutant of VARC 1–291. All VARC constructs were expressed in B834 cells and purified using Ni^{2+}-nitrilotriacetic acid affinity columns by virtue of their C-terminal hexahistidine tags. The best fractions from affinity chromatography were further purified by anion exchange chromatography on Q-Sepharose and then subjected to size exclusion on a Superdex 75 column from Amersham Biosciences.

Two domains of KAHRP (K1A and K2A) that interact with VARC were PCR-amplified from *P. falciparum* 3D7 cDNA using *Pfu* polymerase and cloned into pET28a vector. These constructs were also expressed in B834 cells and purified on Ni^{2+}-nitrilotriacetic acid affinity columns. The nickel elutes were further purified by cation exchange chromatography on SP-Sepharose and then subjected to gel filtration on a Superdex 200 column.

Immunofluorescence Assays—High titer polyclonal antibodies were raised against VARC 1–291 in mice. Thin smears of mature stage *P. falciparum* were fixed in ice-cold methanol for 20 min. These were blocked with 5% BSA and then incubated with anti-VARC antibody (1:1000) for 1 h. After washing with 1$\times$ PBST, the slides were incubated with anti-mouse antibodies (1:2000) conjugated to fluorescein isothiocyanate for 1 h, and treated with 0.1 μM DAPI for 5 min. Slides were again washed extensively with PBST and mounted using Antifade reagent (Bio-Rad). The labeled parasites were visualized using a fluorescence microscope (Nikon) at $\times$40 magnification.

Culturing of Parasites—*P. falciparum* laboratory strains (3D7, FCR3-CSA, and ITG-ICAM) were cultured in RPMI 1640 (Invitrogen) supplemented with 0.5% Albumax I (Invitrogen) (or 10% heat-inactivated human serum) using O^+ RBCs in an environment containing 5% O_2, 5% CO_2, and 90% N_2. Cultures were synchronized by using 5% sorbitol and 65% Percoll using standard procedures. FCR3-CSA and ITG-ICAM cultures were panned on CSA and ICAM-1, respectively, to maintain their binding phenotypes. Briefly, 10 μg/ml CSA (or ICAM-1) were coated overnight on bacteriological Petri plates at 37 °C in a humidified chamber. Purified trophozoites and schizonts were then incubated with bound CSA for 1 h with intermittent shaking. The unbound parasites were removed by extensive washing with incomplete RPMI, and only bound parasites were cultured further.

Phosphorylation Assays—5 μg of VARC was phosphorylated with uninfected erythrocyte lysates (1 μg of total protein) in kinase buffer (20 mM Tris-HCl, pH 8.0, 2.5 mM $MgCl_2$, and 2.5 mM $MnCl_2$, 1 mM sodium vanadate, and 0.5 mM sodium fluoride supplemented with 5 μCi of [γ-^{32}P]ATP) at 30 °C for 1.5 h. Erythrocyte lysates were prepared according to standard protocols. Briefly, histopaque was used to purify erythrocytes from venous blood collected from healthy human volunteers. Packed RBCs were lysed by adding an equal volume of hypotonic lysis solution (10 mM Tris, pH 8.0, 10 mM NaCl). The membrane fraction was separated from the cytoplasmic fraction by centrifuging the lysed cells at 15,000 rpm in Oakridge tubes (SS34 rotor) and collecting the supernatant (cytoplasmic fraction).

The erythrocyte ghosts were repeatedly washed with cold lysis solution until traces of hemoglobin were no longer visible. Kinase reactions of uninfected RBC cytosol or membranes in the absence of recombinant protein, as relevant, were performed in parallel to act as negative controls. The phosphorylated samples were resolved by 12% SDS-polyacrylamide gel electrophoresis and autoradiographed. Inhibitors (heparin (Sigma) and chondroitin sulfate A (CSA), 4,5,6,7-Tetrabromotriazole (TBB), 2-Dimethylamino-4,5,6,7-tetrabromo-1H-benzimidazole (DMAT), tetrabromocinnamic acid (TBCA), (Calbiochem)) and enhancers (Sigma) were added at the desired final concentrations wherever needed. An in-gel kinase assay was also performed to confirm the identity of the kinase responsible for VARC phosphorylation according to published protocols (18). Recombinant CKII (250 units) and erythrocyte membranes (50 μg of total protein) were electrophoresed on SDS-polyacrylamide (15%) gels co-polymerized with 1 mg/ml VARC 1–291 for the assay. Another gel containing 1 mg/ml BSA was used as a control.

Immunoprecipation of Radiolabeled PfEMP1 from Cultured Parasites—Cultured 3D7 parasites were radiolabeled with 50 μCi/ml ^{35}S-protein labeling mix (12 h postinvasion rings) or [^{32}P]orthophosphate (2 h prior to sample collection). Samples were collected at the specified time points as supernatants of parasite pellets lysed in a buffer containing 50 mM Tris, pH 8.0, 150 mM NaCl, 5 mM EDTA, 1% Triton X-100, and 2% SDS. PfEMP1 was immunoprecipitated (using VARC antibodies) from the above samples in NETT buffer (pH 8.1) using standard protocols, resolved on 6% polyacrylamide gels, dried, and autoradiographed.

Circular Dichroism and Fluorescence Spectroscopy—VARC 1–291 was phosphorylated using commercial casein kinase II (New England Biolabs) according to the manufacturer's instructions. An identical reaction without ATP was also done, and this was used as unphosphorylated VARC sample in these experiments. Phosphorylated and unphosphorylated VARC were buffer-exchanged into 10 mM sodium phosphate buffer, pH 8.0. Far UV CD spectra were recorded on Jasco J810 at 25 °C in a quartz cuvette of 0.2-cm path length between wavelengths 190 and 250 nm, at a scan speed of 200 nm/min over three accumulations. The fluorescence measurements were recorded at room temperature in a PerkinElmer LS 50B spectrometer with the excitation slit of 5 nm and emission slit of 10 nm at a scan speed of 900 nm/min. The intrinsic tryptophan fluorescence spectra of phosphorylated and unphosphorylated proteins were recorded from 310 to 500 nm with excitation at 280 nm. Fluorescence intensities were averaged across four scans.

Chymotrypsin Fingerprinting—A total of 100 μg of VARC 1–291 was phosphorylated using casein kinase II (New England Biolabs) in a 100-μl reaction. An identical reaction without ATP was also performed, and this was used as unphosphorylated VARC sample in the chymotrypsin digestion experiment. A kinase reaction of commercial CKII (in the absence of VARC protein) was used as a control to negate bands corresponding to the enzyme itself. A total of 100 ng of chymotrypsin was added to the 100 μg of VARC and incubated at 37 °C. After the indicated time points, 10 μl of reaction mixture (10 μg of VARC) was taken out from both phosphorylated and unphosphorylated tubes, and digestion was stopped by adding SDS-polyacrylamide gel loading buffer. The samples were boiled, resolved by 15% SDS-PAGE and stained with Coomassie Brilliant Blue R250.

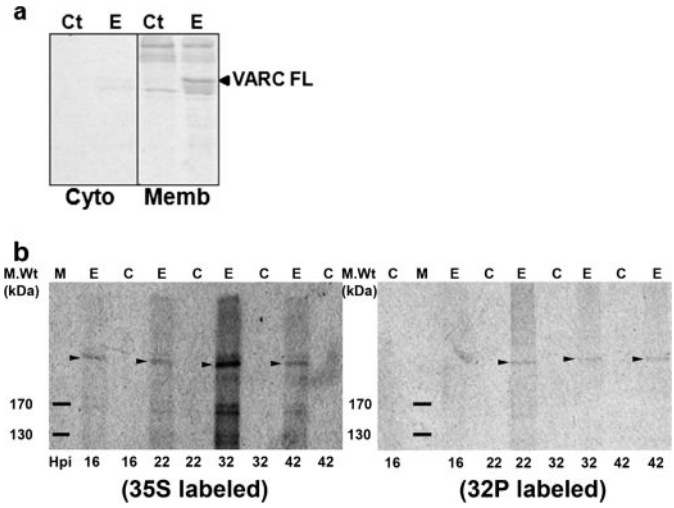

FIGURE 2. **VARC phosphorylation *in vitro* and *in vivo*.** *a*, phosphorylation of VARC FL using erythrocyte cytosol (*Cyto panel*) and membrane (*Memb panel*) as the source of enzyme. 5 μg of recombinant protein was phosphorylated using uninfected erythrocyte lysates (1 μg of total protein each) in kinase buffer (20 mM Tris-HCl, pH 8.0, 2.5 mM $MgCl_2$, 2.5 mM $MnCl_2$, 1 mM sodium vanadate, 0.5 mM sodium fluoride supplemented with 5 μCi of [γ-^{32}P]ATP) at 30 °C for 1.5 h. The phosphorylated samples were resolved by 12% SDS-PAGE and autoradiographed. *Ct*, the reaction minus VARC; *E*, the reaction plus VARC. VARC FL is indicated by an *arrow*, and multiple bands *above* and *below* relate to phosphorylated erythrocyte proteins. *b*, autoradiographs of immunoprecipitated ^{35}S/^{32}P-labeled PfEMP1 resolved by SDS-PAGE at 16, 22, 32, and 42 h postinvasion, as indicated. *M*, protein molecular weight marker; *E*, iRBCs; *C*, uninfected RBCs. Bands corresponding to full-length PfEMP1 are marked by *arrowheads* in either *panel*. Cultured 3D7 parasites were labeled using ^{35}S-protein labeling mix (*^{35}S-labeled panel*) or [^{32}P]orthophosphate (*^{32}P-labeled panel*) as detailed under "Experimental Procedures." Samples were collected 16, 22, 32, and 42 h postinvasion and immunoprecipitated using VARC antibodies in NETT buffer, resolved on 6% SDS-PAGE, and autoradiographed.

Plate-based Protein-Protein Interaction Studies—A total of 100 ng each of K1A, K2A, actin, and spectrin were coated on enzyme-linked immunosorbent assay plates overnight at 4 °C. After blocking with 5% BSA, the coated ligands were allowed to interact with different amounts of VARC FL (commercial CKII phosphorylated *versus* unphosphorylated) in 1× PBS (+2% BSA) for 1 h at 37 °C. The plates were then incubated with anti-VARC antibodies (1:10,000) followed by anti-mouse HRPO (1:20,000) for 1 h each. The plates were developed using 1 mg/ml OPD and H_2O_2 and read at 490 nm.

Static Cytoadherence Assays—Two microliters of CSA (20 μg/ml) or ICAM-1 (25 μg/ml) in PBS were spotted on 60-mm bacteriological Petri plates, allowed to adsorb for 2 h at 37 °C in a humidified chamber, and used for binding assays with parasite cultures. PBS and BSA were spotted as negative controls for both CSA and ICAM-1 binding, whereas CSB and CSC were also used in CSA-binding assays. These plates were then blocked overnight with 1% BSA in PBS at 4 °C. Early to middle trophozoites were treated with 100 μM of either of the CKII inhibitors for 30 min and added to the spotted plates in binding buffer (FCR3-CSA for CSA and ITG-ICAM for ICAM-1, respectively; 1.25 ml at 1% hematocrit, 3% parasitemia). Untreated cultures were used as positive controls to signify 100% binding. The

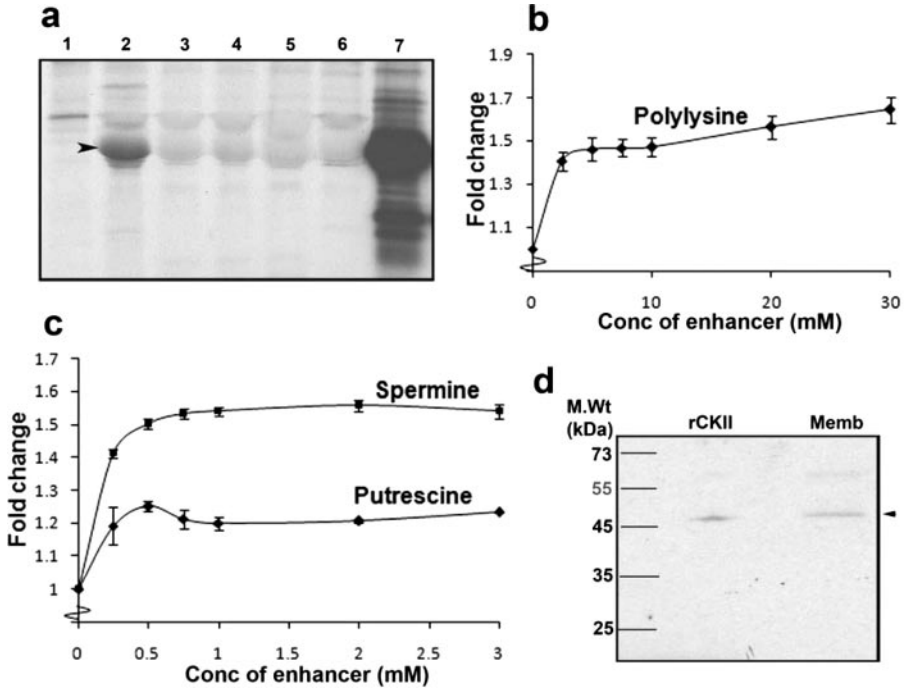

FIGURE 3. **Identification of the kinase responsible for VARC phosphorylation.** *a*, effect of various CKII inhibitors on VARC phosphorylation. Each of these *lanes* shows kinase reactions (with or without inhibitors) using erythrocyte membranes as the source of enzyme, loaded on a 12% SDS-polyacrylamide gel, and autoradiographed. *Lane 1*, reaction minus VARC; *lane 2*, reaction + VARC; *lane 3*, as in *lane 2* + heparin (0.5 μg/ml); *lane 4*, as in *lane 2* + TBB (2 μM); *lane 5*, as in *lane 2* + DMAT (0.5 μM); *lane 6*, as in *lane 2* + TBCA (0.5 μM); *lane 7*, VARC phosphorylation using rCKII (New England Biolabs). *b* and *c*, effect of enhancers (*b*, polylysine; *c*, putrescine and spermine) on VARC phosphorylation. Kinase reactions were performed with the respective concentration of enhancers, loaded on SDS-PAGE, and autoradiographed. Band intensities corresponding to VARC FL were measured using Image J software. -Fold change was calculated considering band intensity of the reaction without any enhancer as 1. The *y* axis depicts the -fold change in phosphorylation, whereas the *x* axis depicts the concentration of enhancer used. All experiments in *b* and *c* were performed three times in triplicate, and the data here are represented as an average of the same. *d*, in-gel kinase assay to confirm the identity of the kinase that phosphorylates VARC. VARC was co-polymerized (1 mg/ml) in a 15% SDS-polyacrylamide gel; rCKII and erythrocyte membranes were resolved on this gel. An in-gel kinase reaction, followed by autoradiography revealed a radioactive band of ~45 kDa in the erythrocyte membrane (*lane Memb*); this corresponds to the size of recombinant CKII catalytic subunit α (*lane rCKII*).

plates were rocked intermittently at 37 °C for 1 h, and unbound erythrocytes were washed away with binding buffer. Bound erythrocytes were fixed in 1% glutaraldehyde for 20 min, stained with 2% Giemsa for 20 min, and scored using a Nikon microscope with a 10× objective. Bound cells were counted from six randomly selected distinct fields in triplicate spots from three independent experiments. Results were expressed as percentage binding in comparison with positive control (no inhibitors added).

Flow-based Cytoadherence Assays—Microslides were coated for 2 h at 37 °C with ICAM-1 (25 μg/ml) or CSA (20 μg/ml) in PBS and blocked overnight with 1% BSA in PBS at 4 °C. Microslides coated with PBS were used as negative controls in these assays. Parasitized RBCs (1% hematocrit and 3% parasitemia) were treated for 30 min with a 100 μM concentration of each of the CKII inhibitors. Untreated parasite cultures were used as positive controls in these experiments to signify 100% binding. These iRBC suspensions were then flowed over receptor-coated microslides for a total of 5 min, and then binding buffer was flowed over to remove unbound cells. The flow rate (0.18 ml/min) yielded a wall shear stress of 0.05 pascals, which has been used widely to mimic wall shear stresses in the microvasculature. The number of stationary or rolling iRBCs was counted in six random fields on the microslides from three independent experiments. Results were expressed as percentage binding in comparison with positive control (no inhibitors added).

RESULTS

Expression and Characterization of Recombinant VARC—Full-length (FL) cytoplasmic C-terminal domain (VARC 1–392) of PfEMP1 (PF08_0141) was cloned and expressed in a bacterial overexpression system and purified to homogeneity (Fig. 1*a*). Recombinant FL VARC (45 kDa) is a dimer in solution, as shown by gel permeation chromatography (Fig. 1*c*). It migrates between BSA dimer (132 kDa) and BSA monomer (66 kDa) on an S200 Superdex column. Due to its flexible nature, the purified protein degrades rapidly. Disorder prediction servers (DisoPred) predict the first 100 and the last 100 amino acids of FL VARC to be highly unstable. Therefore, the VARC 1–291 construct was generated (Fig. 1*a*; this construct was relatively more stable), and polyclonal serum was raised against purified VARC 1–291 in mice. Immunofluorescence assays on cultured 3D7 parasites using these antibodies showed a ring fluorescence pattern characteristic of PfEMP1 protein (Fig. 1*d*).

Phosphorylation of PfEMP1 in Vitro and in Vivo—Since VARC is exposed to the erythrocyte cytoplasm after being transported to the RBC membrane, we tested the ability of erythrocyte kinases to phosphorylate FL VARC. Uninfected RBC extracts (cytosol and membrane; 1 μg of total protein each) were used as the source of enzyme in *in vitro* kinase assays. The membrane fraction of RBCs (Fig. 2a, *lane E*, *Memb panel*) could phosphorylate VARC significantly better than the cytoplasmic fraction (Fig. 2*a*, *lane E*, *cyto panel*) in these kinase reactions, as indicated by the intensity of the band corresponding to recombinant VARC. Since the enzyme responsible for phosphorylation of VARC was present in the erythrocyte membrane at a higher concentration, all *in vitro* phosphorylation reactions involving RBC extracts were hereafter performed using purified erythrocyte membranes. The phosphorylation state of PfEMP1 was tested in cultured 3D7 parasites by radioactive labeling using [^{32}P]orthophosphate, followed by immunoprecipitation of PfEMP1 with VARC antibodies. In order to detect expression of PfEMP1, ^{35}S-labeled parasites were used as a control. Radioactive bands corresponding to the size of full-length PfEMP1 could be observed 22, 32, and 42 h postinvasion (Fig. 2*b*, *^{32}P-labeled panel*), confirming the phosphorylation potential of PfEMP1 *in vivo*. Expression of

PfEMP1 was detectable at all four time points when samples were collected (Fig. 2*b*, ^{35}S-*labeled panel*).

Identification of the Kinase Responsible for Phosphorylation of VARC—A number of inhibitors were used in kinase reactions using erythrocyte membrane as the source of enzyme to identify the kinase responsible for VARC phosphorylation. Staurosporine, a generic Ser/Thr kinase inhibitor, and specific CKII inhibitors (heparin (19), TBB, DMAT, and TBCA) were found to be effective against VARC phosphorylation (Fig. 3*a*) (data not shown for staurosporine). Also, various polyamines (polylysine, putrescine, and spermine) that act as specific enhancers of CKII activity (20) could increase the extent of phosphorylation of VARC in kinase reactions by 25–60%, characteristic of these molecules (20) (Fig. 3, *b* and *c*). An in-gel kinase assay identified a protein band of ~45 kDa (Fig. 3*d*, *lane Memb*) from erythrocyte membranes to be responsible for the phosphorylation function; this corresponds to the size of catalytic subunit α of CKII (Fig. 3*d*, *lane rCKII*). The control gel (co-polymerized with BSA) highlighted no radioactive bands (data not shown), ruling out autophosphorylation of detected bands.

Identification of Sites for CKII-mediated Phosphorylation of VARC—Bioinformatics-based analysis (using phosphorylation and kinase prediction servers) of VARC suggested the presence of several CKII target sites with high scores in the protein. Multiple sequence alignment (ClustalW) of VARCs from 3D7 was used to check which of these sites were conserved among PfEMP1s (Fig. 4*a*). These analyses revealed Thr^{61}, Thr^{64}, Ser^{65}, Ser^{66}, Ser^{68}, and Thr^{328} as the most probable target residues for phosphorylation events. In order to verify these results and determine CKII target sites, two other deletion constructs (residues 87–291 and 87–392) (Fig. 1*b*) were made. Phosphorylation of each of these constructs using erythrocyte membrane as the

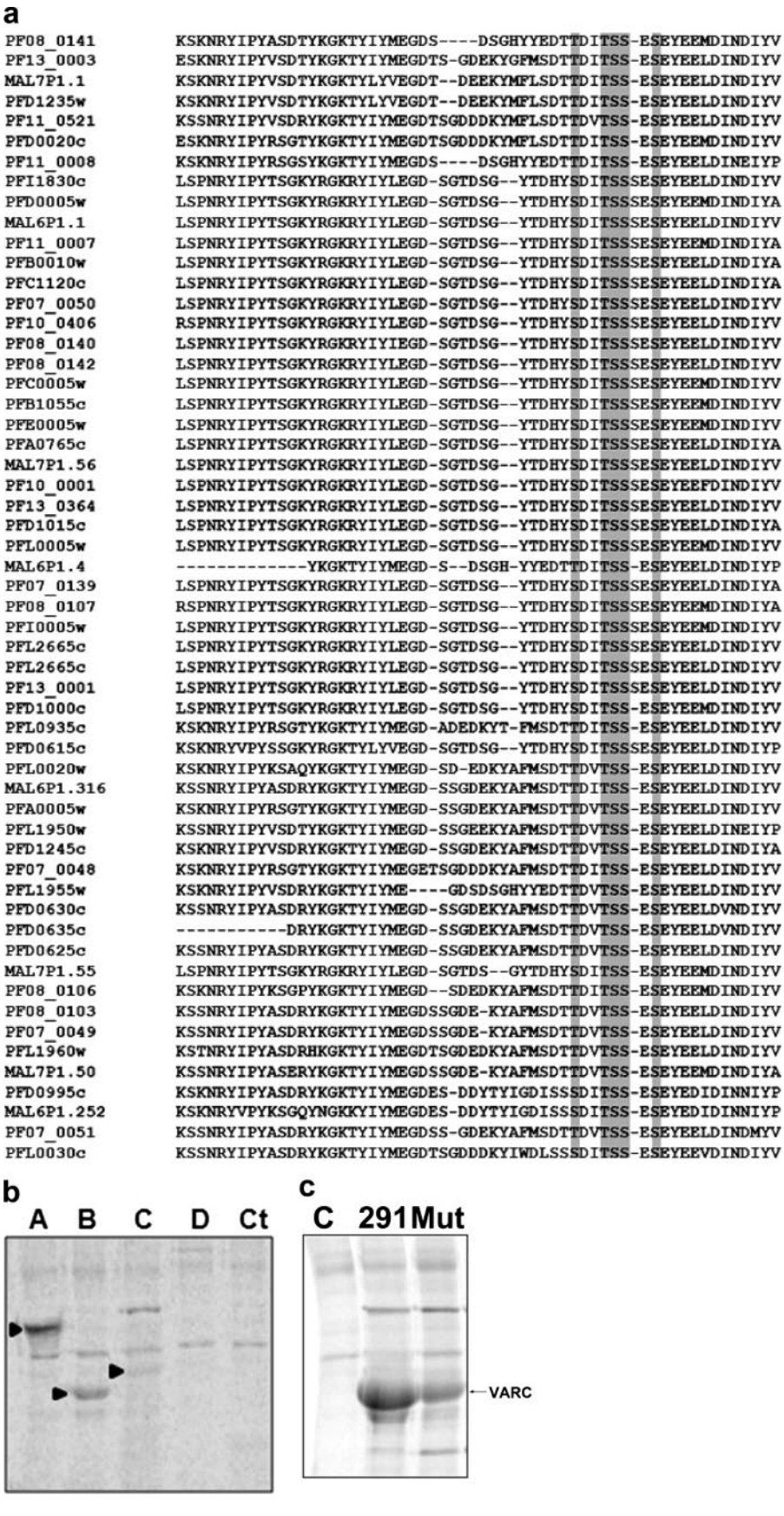

enzyme source in kinase reactions was performed, and the samples were resolved on SDS-PAGE. Our results show that VARC FL and VARC 1–291 could get heavily phosphorylated (Fig. 4*b*, *lanes A* and *B*), whereas VARC 87–291 showed no phosphorylation (Fig. 4*b*, *lane D*). In *lane C*, a faint radioactive band corresponding to the size of VARC 87–392 could be observed (Fig. 4*b*). These findings suggest that the CKII target sites are largely clustered in the first 87 residues of VARC (Thr^{61}, Thr^{64}, Ser^{65}, Ser^{66}, and Ser^{68}), along with Thr^{328} being a likely target. Phosphorylation of a mutant VARC 1–291, where Thr^{61}, Thr^{64}, Ser^{65}, Ser^{66}, and Ser^{68} were changed to alanine by site-directed mutagenesis, showed significant reduction in its phosphorylation potential when tested in an *in vitro* kinase assay (Fig. 4*c*), underscoring the importance of this cluster in VARC modification.

Effect of Phosphorylation on VARC Conformation—CD spectroscopy studies were performed to study the changes in secondary structure of VARC 1–291 upon phosphorylation (Fig. 5*a*). Characteristic spectra of a protein containing both β sheets and random coils were obtained. Comparison of CD spectra of unphosphorylated and phosphorylated VARC (using commercial CKII) suggested that very small and subtle conformational changes occur in VARC 1–291 upon kinase treatment (Fig. 5*a*). The intrinsic tryptophan fluorescence of VARC 1–291 (has four tryptophans) in its phosphorylated and unphosphorylated states was also measured. Fluorescence was enhanced and red shifted (minor) in the case of phosphorylated VARC 1–291, suggesting solvent exposure of previously buried tryptophans in response to phosphorylation (Fig. 5*b*). Mild proteolysis of phosphorylated and unphosphorylated VARC 1–291 using chymotrypsin produced several polymorphic bands (Fig. 5*c*), again suggesting the likelihood of minor structural changes. As shown in Fig. 5*c*, bands 2 and 3 at the 5 min time point and their corresponding bands at further time points are indicative of a domain rearrangement. The appearance of bands 1, 4, and 5 at various time points suggests that structural changes occur in VARC due to phosphorylation.

Strength of VARC Interaction with P. falciparum-encoded Proteins Is Altered by Its Phosphorylation—K1A and K2A are domains of KAHRP that strongly interact with VARC (12). The interaction of FL VARC *versus* commercial CKII-phosphorylated FL VARC was quantitatively measured with each of these KAHRP domains in plate-based binding assays. Phosphorylated FL VARC bound significantly better to both K1A and K2A, as compared with its unphosphorylated form (Fig. 6, *a* and *b*). Although K2A interaction seemed to reach saturation at higher concentrations of phosphorylated VARC, K1A binding to both forms of VARC remained appreciably different even at higher concentrations (Fig. 6, *a* and *b*). Since PfEMP1 is tethered to the RBC cytoskeleton via the binding of its cytoplasmic domain to actin and spectrin, we also studied the effect of FL VARC phosphorylation on its binding to these proteins. The effect of VARC phosphorylation on the interaction of either cytoskeleton proteins with VARC was negligi-

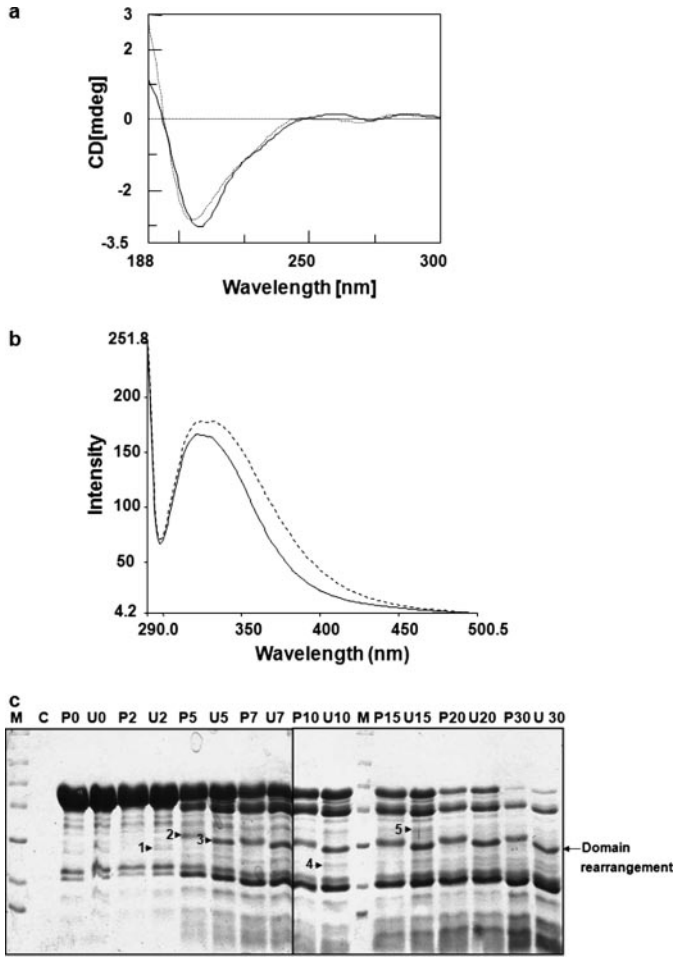

FIGURE 5. **Structural changes in VARC upon phosphorylation.** *a*, far UV CD spectra of phosphorylated and unphosphorylated VARC. VARC 1–291 was phosphorylated with casein kinase II and buffer-exchanged in 10 mM sodium phosphate buffer (pH 8.0). Spectra were recorded on Jasco J810 at 25 °C in a quartz cuvette of 0.2-cm path length between wavelengths 190 and 250 nm, at a scan speed of 200 nm/min over three accumulations, after subtraction of buffer spectra. The spectrum indicated by a *heavy line* corresponds to unphosphorylated VARC, whereas the spectrum indicated with a *dotted line* corresponds to phosphorylated VARC. *b*, tryptophan fluorescence spectra of phosphorylated and unphosphorylated VARC. The intrinsic tryptophan fluorescence spectra of phosphorylated and unphosphorylated proteins were recorded from 310 to 500 nm with excitation wavelength at 280 nm. Fluorescence intensities are the average of four scans. The spectrum indicated by a *heavy line* corresponds to unphosphorylated VARC, whereas the spectrum indicated with a *dotted line* corresponds to phosphorylated VARC. *c*, chymotryptic fingerprinting of phosphorylated VARC. This digestion was performed for indicated times in identical sets for phosphorylated and unphosphorylated VARC, as indicated under "Experimental Procedures." *Lanes labeled U* and *P* represent unphosphorylated and phosphorylated VARC, respectively, followed by the indicated time point (min). *Lane C*, a control for casein kinase II digestion with chymotrypsin. *Arrows 1*, *4*, and *5* indicate the appearance of new bands, whereas *arrows 2* and *3* suggest domain rearrangement in response to phosphorylation.

FIGURE 4. **Identification of CKII target sites on VARC.** *a*, multiple sequence alignment (ClustalW) of VARCs from 3D7 strain of *P. falciparum*. The *gray boxes* show conservation of probable target site residues Thr^{61}, Thr^{64}, Ser^{65}, Ser^{66}, and Ser^{68}. Thr^{328} (not shown) was also conserved. *b*, phosphorylation of VARC constructs (5 μg) with erythrocyte membrane extracts resolved on 12% SDS-PAGE and autoradiographed. *A*, VARC full-length; *B*, VARC 1–291; *C*, VARC 87–392; *D*, VARC 87–291. *Ct*, kinase reaction minus VARC. Positions of phosphorylated VARC bands are indicated by *arrowheads* in the respective *lanes*. *c*, phosphorylation of alanine site-directed mutant of VARC 1–291 at target sites Thr^{61}, Thr^{64}, Ser^{65}, Ser^{66}, and Ser^{68} as compared with that of wild type VARC 1–291. *C*, reaction minus VARC; *291*, reaction + VARC 1–291 (wild type); *Mut*, reaction + mutant VARC.

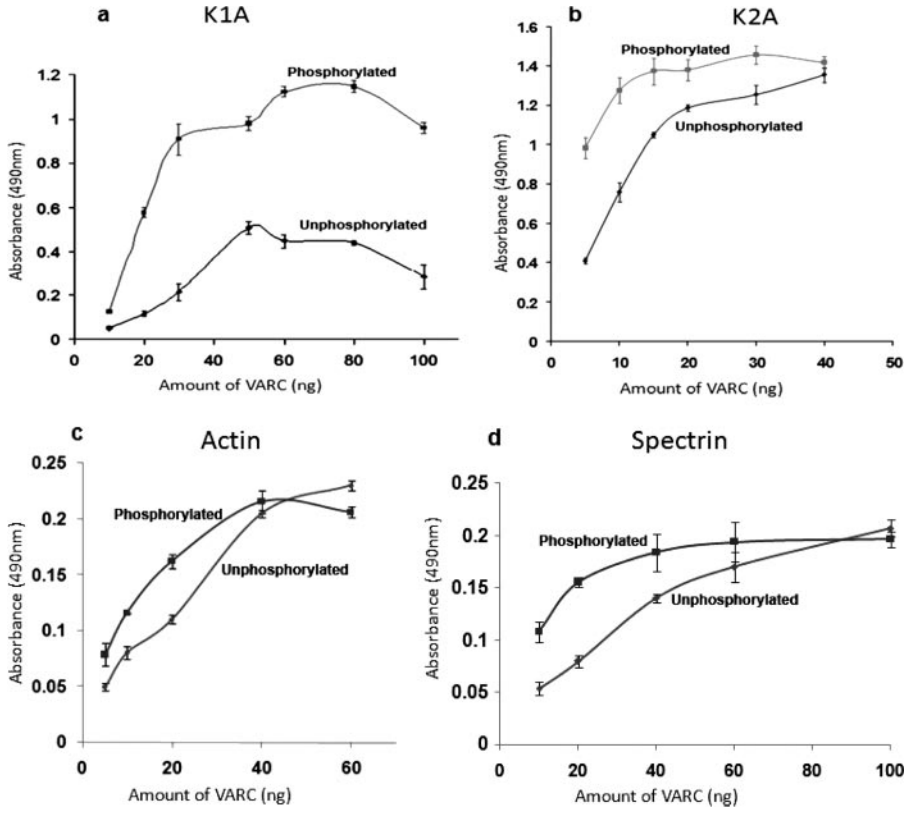

FIGURE 6. **Effect of VARC phosphorylation on its interaction with parasite and host proteins.** Binding of different amounts of unphosphorylated and phosphorylated VARC to K1A (*a*), K2A (*b*), actin (*c*), and spectrin (*d*) is shown. 100 ng of individual proteins K1A, K2A, actin, and spectrin were coated on enzyme-linked immunosorbent assay plates and allowed to interact with different amounts of phosphorylated and unphosphorylated VARC. Concentration-dependent binding curves were plotted, as indicated. The *y* axis represents binding (measured as absorbance at 490 nm), whereas the *x* axis represents VARC concentration (unphosphorylated or phosphorylated, as indicated on the respective *curves*). Each experiment was performed in triplicate, and the average of three experiments was plotted after deducting background signal from the negative control (BSA). The *error bars* represent the S.D. among the three replicates.

ble, as depicted by the contiguous concentration-dependent binding curves (Fig. 6, *c* and *d*).

CKII Inhibition Affects Cytoadherence in Cultured Parasites—Since phosphorylation of VARC increases its affinity for KAHRP domains and VARC-KAHRP interaction has been considered as an important parameter in cytoadherence, we tested the effect of a set of cell-permeable CKII inhibitors on cytoadhesion to soluble endothelial receptors. The binding reduction was scored as follows: 0–25%, low; 25–50%, moderate; >50%, high. The effect of these inhibitors on cytoadherence in static conditions was low to moderate (Fig. 7, *a–c*, *granulated gray bars*) except in the case of TBB on ITG-ICAM (~55% reduction; Fig. 7*a*, *ICAM-1 panel*). However, under flow conditions, the decline in iRBC binding to ICAM-1/CSA in response to CKII inhibitors ranged from moderate to high (Fig. 7, *a–c*, *solid gray bars*).

DISCUSSION

VARCs are the cytoplasmic domains of the PfEMP1 family of proteins, which are unique to *P. falciparum*. These domains are central to the phenomenon of cytoadherence, a major contributor to *P. falciparum* malaria-related deaths. VARCs are likely to be involved in events downstream or upstream of host receptor engagement by the N termini of PfEMP1, making them important and interesting to work on. Here, we have characterized a VARC (PF08_0141) as an example and assigned an important function to these domains. Full-length recombinantly expressed VARC is highly soluble and forms a dimer in solution, as determined by gel permeation chromatography (Fig. 1*c*). Deletion constructs of this domain that are truncated at the amino (residues 87–291 and 87–392) or carboxyl termini (residues 1–291) also run as dimers when subjected to size exclusion (data not shown), implying that the minimal dimerization unit lies within the central portion of the protein. Circular dichroism of full-length VARC revealed that this protein is largely composed of β-sheets and random coils (data not shown).

Since VARCs are cytoplasmic within the RBC, they are likely to serve as an important link between the extracellular cues and erythrocytic responses. Protein phosphorylation constitutes a major mechanism by which cellular processes like metabolism, signal transduction, cell polarity, and cytoskeletal reorganization can be controlled (21). The erythrocyte cytoskeleton is a meshwork of various proteins that interact with each other and regulate important cellular functions. Many RBC membrane proteins are subjected to phosphorylation by the action of erythrocytic kinases (22–25), sometimes even by constitutive association (26). During their growth within the red cells, malaria parasites export a number of their proteins to the RBC membrane (*e.g.* PfEMP1 and KAHRP), which hereafter are treated by the cell as their own (27). This penetration by *Plasmodium* into the host system therefore imparts the parasite exported proteins the ability to interact with erythrocytic molecules (*e.g.* kinases). Keeping this in mind, we tested the phosphorylation potential of VARC *in vitro* using erythrocyte extracts. We found that erythrocyte ghosts could efficiently phosphorylate recombinant full-length and 1–291 VARC, whereas the cytosolic kinases had little effect on VARC (Fig. 2*a*). Modification of a "pseudomembrane" protein by proximal erythrocytic membrane kinases may facilitate the parasites' purpose to undergo phosphorylation. We have also shown that full-length PfEMP1 is phosphorylated *in vivo*. Although expression of this protein can be seen in cultured parasites (^{35}S-labeled) as early as 16 h postinvasion, its phosphorylated form (^{32}P-labeled) is detectable only as the culture progresses to its mature stages (22 h postinvasion onward), when PfEMP1 is exported to the erythrocyte surface (it is widely

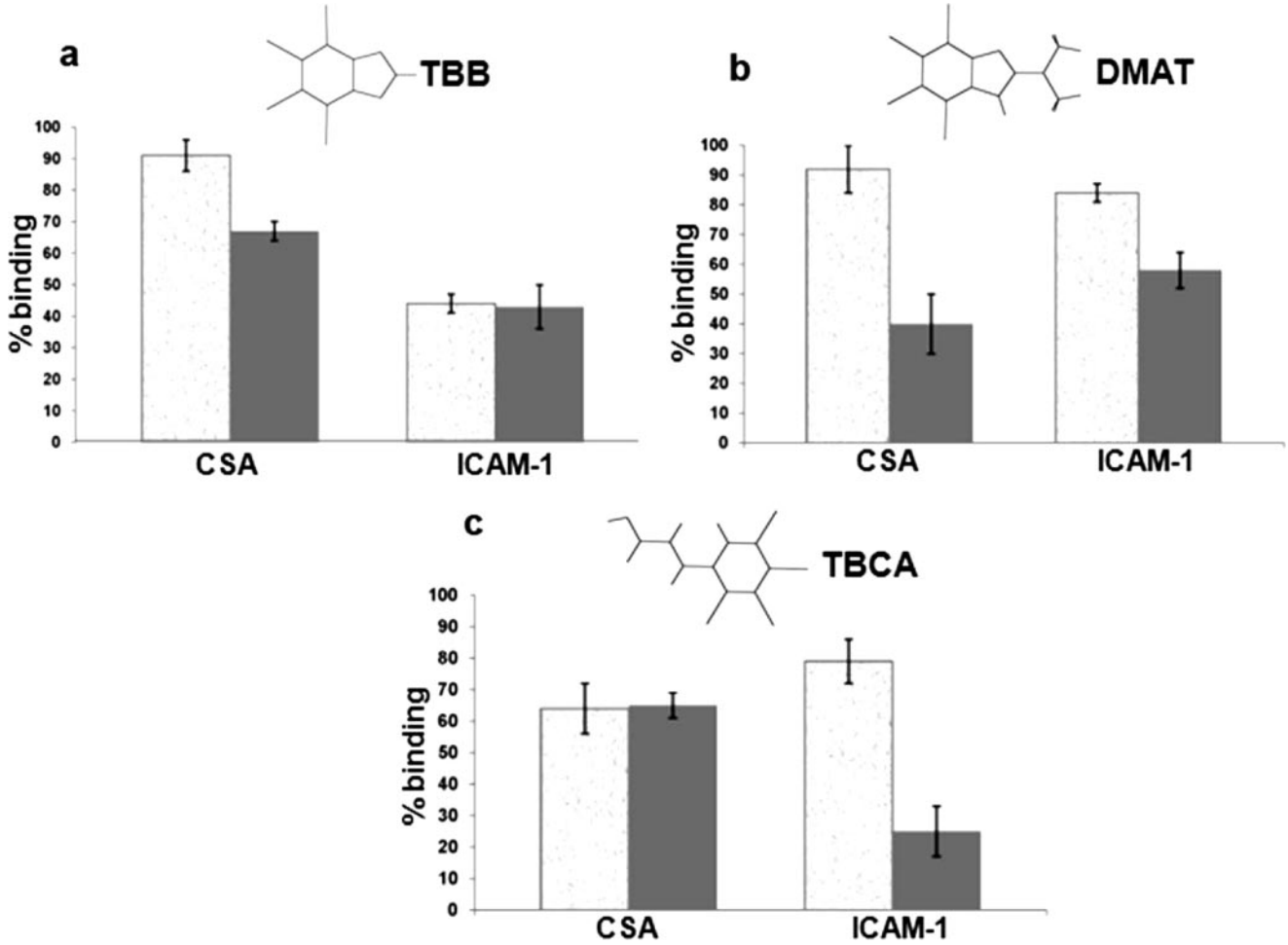

FIGURE 7. **Effect of CKII inhibitors on cytoadherence.** The effect of TBB (*a*), DMAT (*b*), and TBCA (*c*) on binding of FCR3-CSA to CSA (*CSA panels*) and ITG-ICAM to ICAM-1 (*ICAM-1 panels*). Parasitized RBCs were treated for 30 min with a 100 μM concentration of each of the CKII inhibitors, as indicated. iRBC suspensions (1% hematocrit and 3% parasitemia) were flowed over receptor-coated microslides for 5 min. The flow rate was set to 0.18 ml/min. The number of stationary or rolling iRBCs was counted in six random fields on the microslides from three independent experiments. Results were expressed as percentage binding in comparison with untreated culture (100% binding). Microslides coated with PBS were used as negative controls in these assays. *Granulated gray bars* represent data from static assays, whereas *solid gray bars* represent data from flow assays.

believed that export of PfEMP1 to RBC surface is effected in the 16–20 h postinvasion window (Fig. 2*b*).

We have identified CKII as the enzyme responsible for this post-translational modification by using specific inhibitors {heparin (19), TBB, DMAT, and TBCA} and enhancers (polyamines) (20) in kinase assays (Fig. 3, *a*–*c*). Polyamines like spermine, putrescine, and polylysine are known to stimulate CKII by causing an aggregation of the substrate, thereby increasing its effective concentration (28). An in-gel kinase assay for VARC to identify the responsible enzyme (in erythrocyte membranes) highlights a band corresponding to the size of the catalytic subunit α of CKII (Fig. 3*d*). This enzyme is a ubiquitously expressed (in all tissues and organisms) and probably constitutively active Ser/Thr kinase that is located in nearly all subcellular compartments (29). The erythrocyte membrane has a distinct pool of CKII, which along with the cytosolic pool phosphorylates most of the cytoskeletal proteins, including spectrin, ankyrin, and adducin (23, 26, 30). Our bioinformatics analysis to identify the target residues for phosphorylation along with the kinasing data of N- and C-terminal deletion constructs suggests that most CKII target sites on VARC exist in an N-terminal acidic cluster, typical of CKII recognition sites (Fig. 4, *a* and *b*). A variant of VARC 1–291, where the N-terminal acidic cluster has been mutated by alanine site-directed mutagenesis, shows significantly reduced phosphorylation capability in kinase assays using erythrocyte membranes (Fig. 4*c*). Another isolated residue of VARC that is likely to undergo phosphorylation is Thr^{328}, which lies on its C terminus. Our results imply that VARC harbors multiple phosphorylation sites for its modification within the RBC. CKII-mediated phosphorylation of various proteins is known to change their conformation upon modification (31, 32). Our data suggest that VARC undergoes subtle conformational alterations upon phosphorylation (Fig. 5).

Phosphorylation of erythrocyte cytoskeletal proteins alters their binding affinity for each other, which has important implications in cellular function (23, 26, 30). VARC is known to tether PfEMP1 to the RBC cytoskeleton by interacting with host proteins actin and spectrin and parasite encoded KAHRP. Here, we have shown that phosphorylation of VARC has a considerable impact on its interaction with KAHRP domains K1A and K2A, whereas the effect on resident host proteins (actin

and spectrin) is negligible. Our results depict that upon phosphorylation of VARC, its binding to K1A was altered more dramatically than to K2A (Fig. 6, *a* and *b*). Since K1A interacts with the C terminus of VARC, it is probable that Thr^{328} phosphorylation confers a greater structural change in VARC, as opposed to modification of the N terminus, which is known to bind K2A. Although spectrin is also a substrate for CKII *in vivo*, we have observed that its phosphorylation does not have any effect on VARC-spectrin association (data not shown).

Previous reports suggest that VARC-KAHRP interaction is central to cytoadherence. Therefore, a change in their binding strength for each other is likely to reflect on how well iRBCs cytoadhere. We have studied cytoadhesion abilities of cultured parasites treated with commercially available, cell-permeable, and specific CKII inhibitors (33). All three inhibitors used in this study reduce CKII mediated phosphorylation by competing for the enzyme's ATP binding pocket. The effect of these inhibitors on cytoadherence in static conditions was mostly insignificant (Fig. 7, *a* (*CSA panel*), *b*, and *c*), with the exception of TBB on ITG-ICAM (~55% reduction; Fig. 7*a*, *ICAM-1 panel*). However, under flow conditions, the decline in iRBC binding to ICAM-1/CSA in response to CKII inhibitors was significant (Fig. 7, *a*–*c*). Notably, TBCA reduces binding on ICAM-1 by 75% (Fig. 7*c*), DMAT on CSA by 65% (Fig. 7*b*), and TBB on ICAM-1 by 55% (Fig. 7*a*). Binding of PfEMP1s to host receptors like CSA and ICAM-1 is considered important in severe placental and cerebral malaria, respectively. Our data show that CKII inhibition causes parasitized RBCs to cytoadhere more weakly to soluble receptors under flow conditions, as compared with static conditions. On the basis of these results, we propose the following. Due to a decline in VARC phosphorylation and hence weaker binding to KAHRP, it is probable that PfEMP1 is inadequately anchored to the erythrocyte cytoskeleton, impairing cytoadherence in circulation. On the other hand, binding of PfEMP1s to their respective host endothelial receptors is not challenged in the absence of physiological shear stress (*i.e.* static assays). Due to the universal requirement of CKII in cellular functions, one could argue that the enzyme's inhibition could be lethal to the parasite. However, the capability of dead parasites to cytoadhere equals that of live parasites.[3] Nonetheless, a possibility that CKII inhibition produces a more generic effect on iRBC morphology to alter their cytoadherence properties cannot be ruled out.

Due to polyamine biosynthesis or increased uptake of putrescine from the extracellular pool (34, 35), mature stage iRBCs have significantly elevated levels of polyamines as compared with uninfected or ring stage parasites. This probably acts in favor of parasites so that they can utilize their resources to increase VARC phosphorylation and cytoadhere better in order to evade host response. The presence of several polylysine stretches in KAHRP may be a parasite's evolutionary attempt to enhance VARC phosphorylation and strengthen its roots.

Phosphorylation of major cytoskeletal proteins, such as ankyrin, band 4.1, and band 4.9, can weaken the rigidity of the cytoskeleton by reducing the binding affinity of these components (24, 26). This property of the erythrocytes is extremely important, since it regulates membrane deformability essential for passage through microvasculature. Although the precise mechanisms leading to decreased deformability of iRBCs are poorly understood, the contribution of parasite proteins to increased membrane rigidity is most likely attributable to their direct or indirect interactions with proteins of the RBC membrane skeleton or other exported parasite proteins (36, 37). Since phosphorylation of VARC increases its affinity for KAHRP, it could be one of the factors for increased membrane rigidity of *P. falciparum*-infected RBCs.

Since cytoadhesion is a major mechanism by which *P. falciparum* implements its pathophysiology, drugs that potentially diminish cytoadherence are considered important agents in the fight against virulent malaria. This is the first report where small molecule CKII inhibitors have been assessed for their anti-cytoadherence activity by targeting intracellular events. This study suggests that molecules that block or reverse the interaction between VARC and its binding partners have the ability to reduce cytoadherence and may therefore be effective against severe malaria. The CKII target site on VARC presents itself as a potential new target for development of anti-cytoadherence agents. Finally, therapeutics that act to suppress the molecular functions of conserved VARCs are likely to have an edge over the ones that aim at abrogating the variable extracellular PfEMP1-host receptor interactions.

[3] A. Craig, unpublished data.

REFERENCES

1. Snow, R. W., Guerra, C. A., Noor, A. M., Myint, H. Y., and Hay, S. I. (2005) *Nature* **434,** 214–217
2. Smith, J. D., Chitnis, C. E., Craig, A. G., Roberts, D. J., Hudson-Taylor, D. E., Peterson, D. S., Pinches, R., Newbold, C. I., and Miller, L. H. (1995) *Cell* **82,** 101–110
3. Su, X. Z., Heatwole, V. M., Wertheimer, S. P., Guinet, F., Herrfeldt, J. A., Peterson, D. S., Ravetch, J. A., and Wellems, T. E. (1995) *Cell* **82,** 89–100
4. Baruch, D. I., Pasloske, B. L., Singh, H. B., Bi, X., Ma, X. C., Feldman, M., Taraschi, T. F., and Howard, R. J. (1995) *Cell* **82,** 77–87
5. Barnwell, J. W., Asch, A. S., Nachman, R. L., Yamaya, M., Aikawa, M., and Ingravallo, P. (1989) *J. Clin. Invest.* **84,** 765–772
6. Barragan, A., Spillmann, D., Carlson, J., and Wahlgren, M. (1999) *Biochem. Soc. Transact.* **27,** 487–493
7. Berendt, A. R., Simmons, D. L., Tansey, J., Newbold, C. I., and Marsh, K. (1989) *Nature* **341,** 57–59
8. Oh, S. S., Voigt, S., Fisher, D., Yi, S. J., LeRoy, P. J., Derick, L. H., Liu, S., and Chishti, A. H. (2000) *Mol. Biochem. Parasitol.* **108,** 237–247
9. Crabb, B. S., Cooke, B. M., Reeder, J. C., Waller, R. F., Caruana, S. R., Davern, K. M., Wickham, M. E., Brown, G. V., Coppel, R. L., and Cowman, A. F. (1997) *Cell* **89,** 287–296
10. Culvenor, J. G., Langford, C. J., Crewther, P. E., Saint, R. B., Coppel, R. L., Kemp, D. J., Anders, R. F., and Brown, G. V. (1987) *Exp. Parasitol.* **63,** 58–67
11. Pologe, L. G., Pavlovec, A., Shio, H., and Ravetch, J. V. (1987) *Proc. Natl. Acad. Sci. U. S. A.* **84,** 7139–7143
12. Waller, K. L., Cooke, B. M., Nunomura, W., Mohandas, N., and Coppel, R. L. (1999) *J. Biol. Chem.* **274,** 23808–23813
13. Waller, K. L., Nunomura, W., Cooke, B. M., Mohandas, N., and Coppel, R. L. (2002) *Mol. Biochem. Parasitol.* **119,** 125–129
14. Voigt, S., Hanspal, M., LeRoy, P. J., Zhao, P. S., Oh, S. S., Chishti, A. H., and Liu, S. C. (2000) *Mol. Biochem. Parasitol.* **110,** 423–428
15. Berendt, A. R., Ferguson, D. J., Gardner, J., Turner, G., Rowe, A., McCormick, C., Roberts, D., Craig, A., Pinches, R., and Elford, B. C. (1994) *Parasitology* **108,** (suppl.) 19–28

16. Ruangjirachuporn, W., Afzelius, B. A., Paulie, S., Wahlgren, M., Berzins, K., and Perlmann, P. (1991) *Parasitology* **102,** 325–334
17. Horrocks, P., Pinches, R. A., Chakravorty, S. J., Papakrivos, J., Christodoulou, Z., Kyes, S. A., Urban, B. C., Ferguson, D. J., and Newbold, C. I. (2005) *J. Cell Sci.* **118,** 2507–2518
18. Kameshita, I., and Fujisawa, H. (1989) *Anal. Biochem.* **183,** 139–143
19. Hathaway, G. M., Lubben, T. H., and Traugh, J. A. (1980) *J. Biol. Chem.* **255,** 8038–8041
20. Hathaway, G. M., and Traugh, J. A. (1984) *J. Biol. Chem.* **259,** 7011–7015
21. Cohen, P. (2002) *Nat. Cell Biol.* **4,** E127–E130
22. Brunati, A. M., Bordin, L., Clari, G., James, P., Quadroni, M., Baritono, E., Pinna, L. A., and Donella-Deana, A. (2000) *Blood* **96,** 1550–1557
23. Fukata, Y., Oshiro, N., Kinoshita, N., Kawano, Y., Matsuoka, Y., Bennett, V., Matsuura, Y., and Kaibuchi, K. (1999) *J. Cell Biol.* **145,** 347–361
24. Ling, E., Danilov, Y. N., and Cohen, C. M. (1988) *J. Biol. Chem.* **263,** 2209–2216
25. Wagner, L. M., Fowler, V. M., and Takemoto, D. J. (2002) *Mol. Vision* **8,** 394–406
26. Ghosh, S., Dorsey, F. C., and Cox, J. V. (2002) *J. Cell Sci.* **115,** 4107–4115
27. Marti, M., Good, R. T., Rug, M., Knuepfer, E., and Cowman, A. F. (2004) *Science* **306,** 1930–1933
28. Lechuga, M. T., Moreno, V., Pelegrina, S., Gomez-Ariza, C. J., and Bajo, M. T. (2006) *Acta Psychol.* **123,** 279–298
29. Faust, M., and Montenarh, M. (2000) *Cell Tissue Res.* **301,** 329–340
30. Patel, V. P., and Fairbanks, G. (1981) *J. Cell Biol.* **88,** 430–440
31. Penrose, K. J., Garcia-Alai, M., de Prat-Gay, G., and McBride, A. A. (2004) *J. Biol. Chem.* **279,** 22430–22439
32. Raha, T., Samal, E., Majumdar, A., Basak, S., Chattopadhyay, D., and Chattopadhyay, D. J. (2000) *Protein Eng.* **13,** 437–444
33. Sarno, S., Salvi, M., Battistutta, R., Zanotti, G., and Pinna, L. A. (2005) *Biochim. Biophys. Acta* **1754,** 263–270
34. Assaraf, Y. G., Golenser, J., Spira, D. T., and Bachrach, U. (1984) *Biochem. J.* **222,** 815–819
35. Ramya, T. N., Surolia, N., and Surolia, A. (2006) *Biochem. Biophys. Res. Commun.* **348,** 579–584
36. Dondorp, A. M., Kager, P. A., Vreeken, J., and White, N. J. (2000) *Parasitol. Today* **16,** 228–232
37. Glenister, F. K., Coppel, R. L., Cowman, A. F., Mohandas, N., and Cooke, B. M. (2002) *Blood* **99,** 1060–1063